



## An Innovative Advanced Oxidation Technology for Effective Decomposition of Formaldehyde by Combining Iron Modified Nano-TiO<sub>2</sub> (Fe/TiO<sub>2</sub>) Photocatalytic Degradation with Ozone Oxidation

Su-Wen Cheng<sup>1</sup>, Yu-Hua Li<sup>2</sup>, Chung-Shin Yuan<sup>1\*</sup>, Pei-Yi Tsai<sup>1</sup>, Hua-Zhen Shen<sup>3</sup>,  
Chung-Hsuang Hung<sup>4</sup>

<sup>1</sup> Institute of Environmental Engineering, National Sun Yat-Sen University, Kaohsiung 80424, Taiwan

<sup>2</sup> School of Resources and Environmental Science, Hubei University, Wuhan 430068, China

<sup>3</sup> College of Chemical Engineering, Huaqiao University, Xiamen 362021, China

<sup>4</sup> Department of Safety, Health and Environmental Engineering, National Kaohsiung University of Science and Technology, Kaohsiung 81164, Taiwan

---

### ABSTRACT

Bench-scale experiments using iron modified and unmodified photocatalysts (Fe/TiO<sub>2</sub> and TiO<sub>2</sub>) were conducted to compare their decomposition efficiencies with formaldehyde. The effects of operating parameters on the decomposition efficiency were further investigated. The grain size of iron doped photocatalysts ranged from 25 to 60 nm. The iron doped content of 1, 3, and 5% Fe/TiO<sub>2</sub> photocatalysts was measured as 1.2, 3.1, and 4.7%, respectively. The UV-visible analytical results showed that a significant red shift was observed while the iron doping content of Fe/TiO<sub>2</sub> increased from 0 to 5%. Two continuous-flow reaction systems, the ozonolytic and the photocatalytic reactors, were combined in series to investigate their capability to decompose formaldehyde by Fe/TiO<sub>2</sub> photocatalysts with six operating parameters, namely, the influent formaldehyde concentrations (0.15, 0.30, and 0.45 ppm), the relative humidity (5, 35, and 55%), irradiation by light (visible, near-UV, and UV), the reaction temperatures (25, 30, and 35°C), the iron doping content (1, 3, and 5% Fe/TiO<sub>2</sub>), and the injected-ozone concentrations (2,000 and 3,000 ppb). The optimal operating parameters obtained in this study were an influent formaldehyde concentration of 0.15 ppm, a relative humidity of 5%, irradiation by UV light, a reaction temperature of 35°C, an iron doping content of 5% Fe/TiO<sub>2</sub>, and an injected-ozone concentration of 3,000 ppb. Overall, the efficiencies of different decomposition techniques for formaldehyde followed the sequence: UV/TiO<sub>2</sub> + O<sub>3</sub> > O<sub>3</sub> + UV/TiO<sub>2</sub> > UV/O<sub>3</sub> ≈ O<sub>3</sub>. A maximum formaldehyde decomposition efficiency of 92% was obtained by using the UV/TiO<sub>2</sub> + O<sub>3</sub> technology.

**Keywords:** Indoor formaldehyde; Fe/TiO<sub>2</sub> photocatalyst; Ozonolysis; Decomposition efficiency of formaldehyde; Operating parameters.

---

### INTRODUCTION

In recent years, people spend more than 80% of their time in indoor environments, and even higher than 90% in urban areas (Zeliger, 2011). Numerous studies have been conducted to characterize the poor indoor air quality in the office and residential environments causing sick building syndrome (SBS), sick house syndrome (SHS), and multiple chemical sensitivity (MCS) (Jones, 1999). Among the indoor air pollutants, formaldehyde is a carcinogenic VOC

causing severe adverse effects on human health (Jones, 1999; Chin *et al.*, 2006; Zeliger, 2011; Kwon *et al.*, 2015). Indoor Air Quality Management Act of Taiwan has been promulgated on November 23, 2011, and formally implemented on November 23, 2012, which make Taiwan as the second country in the world promoting the indoor air quality management legislation after South Korea. A total of nine air pollutants including carbon dioxide (CO<sub>2</sub>), carbon monoxide (CO), formaldehyde (HCHO), total volatile organic compounds (TVOCs), PM<sub>2.5</sub>, PM<sub>10</sub>, ozone (O<sub>3</sub>), fungi, and bacteria are regulated.

Among the indoor air pollutants, volatile organic compounds (VOCs) are commonly observed in indoor environments. Formaldehyde as a typical carcinogenic VOC could potentially cause cancer and is harmful to human health when uptake into human bodies via inhalation and

---

\* Corresponding author.

Tel.: 886-7-5252000 ext. 4409; Fax: 886-7-5254409

E-mail address: ycsngi@mail.nsysu.edu.tw

skin contact. Therefore, removing formaldehyde from indoor air is an essential measure for improving indoor air quality and protecting human beings (Charuwan *et al.*, 2012; Delphine *et al.*, 2014; Ho *et al.*, 2015). Regarding a large number of indoor VOC sources such as building materials, furniture and decoration, burning of petroleum products, cigarette smoking, electrical appliances, usage of cleaning products and household chemicals, formaldehyde is found to be present at higher concentrations in indoor air than outdoors (Chai and Pawliszyn, 1995). Primary sources of formaldehyde are building and decorating materials such as particleboard, plywood, resins, adhesives, and carpeting (Hines *et al.*, 1993; Hong *et al.*, 2017). It is also commonly applied for the manufacture of urea formaldehyde foam insulation (UFFI) which is injected into wall cavities to supplement the insulation in the existing buildings.

There are three major pathways for formaldehyde entering human body, including skin contact, ingestion, and inhalation. Exposure at low formaldehyde concentrations may cause sneezing, burning sensation in eyes, and upper respiratory allergy, while exposure at high formaldehyde concentrations can cause severe respiratory irritation aggravated including bronchitis, pneumonia, laryngitis, headaches, dizziness, breathing difficulties, pulmonary edema, cough, difficulty swallowing, and even death. Direct exposure at high concentrations of formaldehyde vapor or solution could cause skin whitening; hard, roughened skin; and even coagulation necrosis. Long-term exposure at low concentrations of formaldehyde vapor would cause skin inflammation, allergies, nails break, and ulcers. Direct intake can cause mouth, throat, esophagus and gastrointestinal mucosal surfaces irritation and aggravated pain, and kidney damage, which will affect the central nervous system, causing the symptoms of alcoholism, dizziness, depression, coma symptoms, and even death (Romaguera *et al.*, 1981).

Titanium dioxide ( $\text{TiO}_2$ ) has been widely used as a promising photocatalyst for the elimination of environmental pollutants and is a harmless white powder, which has been proved to be very active in the photo-oxidation of various organic compounds (Alberici *et al.*, 2001). By irradiating suitable lights with wavelengths below 400 nm,  $\text{TiO}_2$  photocatalyst tends to absorb photons and promote photocatalytic redox reactions on its surface (Sano *et al.*, 2000). Semiconductor photocatalysis with a primary focus on  $\text{TiO}_2$  as a durable photocatalyst has been applied to a variety of environmental problems of interest such as water and air purification (Hoffmann *et al.*, 1995).  $\text{TiO}_2$  has been considered as the most promising photocatalyst owing to its photocatalytic reactivity, long-term stability, non-toxic characteristics, and low cost. However, it can only utilize about 4% of solar spectrum in the UV region due to its wide band gap (i.e., 3.20 eV for anatase and 3.00 eV for rutile) (Tao *et al.*, 2015; Xiong *et al.*, 2015).

Increasing interest in semiconductor mediated photocatalysis continues to grow due to the versatile possibility in the utilization of semiconductor photon produced efficient redox equivalents,  $\text{h}^+$  and  $\text{e}^-$ , for various potential chemical reactions. The role of surface modification of various semiconductor materials (e.g.,  $\text{TiO}_2$ , CdS, ZnS,

and ZnO) has been investigated for the enhancement of photocatalytic efficiency (Dhananjeyan *et al.*, 1997). Tang *et al.* (2014) reported that much efforts have been spent in developing single-phase mixed metal oxides which have photocatalytic reactivity in the visible-light wavelength region, such as  $\text{Bi}_2\text{WO}_6$ ,  $\text{BiVO}_4$ , and  $\text{AgAlO}_2$  (Yun *et al.*, 2010; Gao *et al.*, 2011; Xu *et al.*, 2012).

Ozone is an allotrope of oxygen, which is a colorless and non-toxic gas, because ozone has one more oxygen atom compared to oxygen, and therefore has very lively characteristics, also known as reactive oxygen species. Ozone has been commonly used as the strongest natural bactericide. Its bactericidal power is approximately 3,000 times of chlorine and its oxidation capacity is about 600 times of chlorine, which make ozone rank the second to fluorine. Additionally, ozone has strong oxidizing ability when faced with bacteria, mold, toxic chemicals, and smelly taste, which can produce oxidation reactions immediately and play for deodorant, sterilization, and air purification. Ozone could easily dissolve in carbon tetrachloride or fluorocarbons but slightly dissolve in water and thus it is unstable and prone to oxygen reduction reaction.

Although both ozonolytic and photocatalytic oxidation have been widely used to decompose VOCs separately, the combination of ozonolytic and photocatalytic oxidation has not been applied for the removal of VOCs, particularly for formaldehyde. Accordingly, this study aims to develop an innovative advanced oxidation technology (AOT) by combining photocatalytic oxidation with ozonolysis to effectively decompose indoor formaldehyde and investigate the effects of various operating parameters on the decomposition efficiency of formaldehyde.

## EXPERIMENTAL METHODS

### *Photocatalytic and Ozonolytic Oxidation System*

The set-up of a continuous-flow reaction system consisting of a photocatalytic reactor and an ozone reactor is illustrated in Fig. 1. Formaldehyde of fixed concentration was generated by heating a formaldehyde permeation tube at  $50^\circ\text{C}$ , properly mixed with nitrogen gas in a mixing chamber, and then entered into a continuous-flow photocatalytic reactor for decomposing formaldehyde. A 15-watt lamp (UV, near-UV, or visible lights) wrapped with fiberglass coated by iron-doped  $\text{TiO}_2$  ( $\text{Fe}/\text{TiO}_2$ ) photocatalyst was situated inside the photocatalytic reactor. The ozone reactor made of pyrex glass was used to oxidize formaldehyde with the injected ozone produced by an ozone generator. An on-line formaldehyde monitor based on the principle of electrochemistry was then applied to continuously monitor the formaldehyde concentration in the effluent gas.

### *Preparation of $\text{Fe}/\text{TiO}_2$*

A commercial titanium dioxide ( $\text{TiO}_2$ ), Degussa P-25, photocatalyst used in this study has been widely applied for air pollution control, wastewater treatment, water purification, and antibacterial. It was originally mixed with iron oxide to produce modified photocatalysts ( $\text{Fe}/\text{TiO}_2$ ) and then coated on a supporting medium fiberglass. Prior

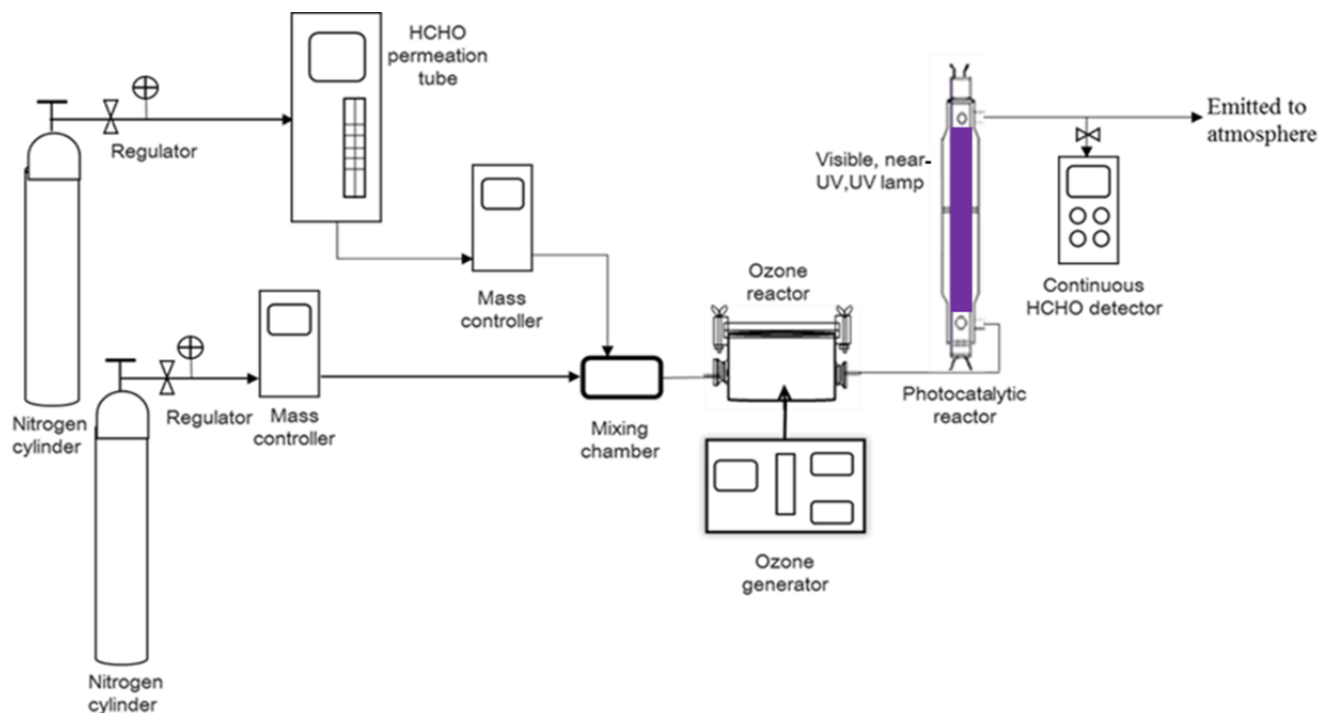


**Fig. 1.** The set-up of a continuous-flow photocatalytic reactor combined with ozone oxidation reactor.

to coating, the fiberglass was temporarily dried in an oven at 105°C for 2 hours to expel impurities from the fiberglass, which was then coated with Fe/TiO<sub>2</sub> photocatalyst by mixing 0.01 g of Degussa P-25 TiO<sub>2</sub> powder with 100 mL of distilled water, and doped by 0.027 g iron Fe<sup>2+</sup> (II) to form a solution of 1, 3, and 5% Fe/TiO<sub>2</sub>. The fiberglass was then impregnated in the Fe/TiO<sub>2</sub> solution for 30 sec and dried in the oven at 105°C for 2 hours.

#### **Characterization of Fe/TiO<sub>2</sub>**

In this study, the surface characteristics of TiO<sub>2</sub> (Degussa P-25) and iron-doped TiO<sub>2</sub> (Fe/TiO<sub>2</sub>) photocatalysts coated on the surface of fiberglass was further analyzed by a scanning electron microscope with an energy dispersive spectrometer (SEM/EDS, Model 6300) to observe the morphology of the fiberglass surface, measure the particle and grain size of the photocatalysts, and further analyze the elemental composition of Fe/TiO<sub>2</sub> photocatalysts. The optical absorption spectra of the photocatalysts were measured in the wavelength range of 200–800 nm by using an UV-Vis spectrophotometer (Jasco, V670). Free radicals were determined with an unpaired electron paramagnetic substance or an electron paramagnetic resonance (EPR) spectroscopy (BRUKER ELEXSYS, series E-580).

#### **Formaldehyde Decomposition Experiments**

This study combined photocatalytic degradation with ozone oxidation technology to decompose formaldehyde and further investigated the decomposition efficiency of formaldehyde with operating parameters. A continuous-flow reaction system was self-designed and installed to conduct the formaldehyde decomposition experiments. The reaction system consisted of a formaldehyde generation

unit, a photocatalytic degradation unit, and an ozone oxidation unit. Fig. 1 depicts the set-up of the continuous-flow reaction system combining the photocatalytic and ozonolytic techniques (UV/TiO<sub>2</sub> + O<sub>3</sub>).

The experimental parameters investigated in this study included the influent formaldehyde concentration (0.15, 0.30, and 0.45 ppm), the relative humidity (5, 35, and 55%), the reaction temperature (25, 30, and 35°C), the wavelength of light irradiation (visible light, near-ultraviolet light, and ultraviolet light), the iron doping content (1, 3, and 5%), and the injection ozone concentration (2,000 and 3,000 ppb). This study further explored the optimal decomposition efficiency of formaldehyde by combining photocatalytic degradation and ozone oxidation techniques in different sequence.

## **RESULTS AND DISCUSSION**

#### **Physical and Chemical Characteristics of Fe/TiO<sub>2</sub> Photocatalysts**

In this study, the iron modified Fe/TiO<sub>2</sub> photocatalysts were initially prepared by the impregnation method. The crystal structure, surface morphology, particle and grain size, and elemental abundance of the modified Fe/TiO<sub>2</sub> photocatalysts were further examined by SEM/EDS. Fig. 2 illustrates the SEM images of TiO<sub>2</sub> and Fe/TiO<sub>2</sub> photocatalysts coated on the surface of the fiberglasses. The grain size of TiO<sub>2</sub>, 1% Fe/TiO<sub>2</sub>, 3% Fe/TiO<sub>2</sub>, and 5% Fe/TiO<sub>2</sub> photocatalysts were 25, 42, 50, and 60 nm, respectively. It showed that the grain size increased with the mass percentage of iron impregnated with TiO<sub>2</sub>. For the EDS analysis of Fe/TiO<sub>2</sub> photocatalysts (see Fig. 3), the iron contents were measured as 1.2, 3.1, and 4.7% for

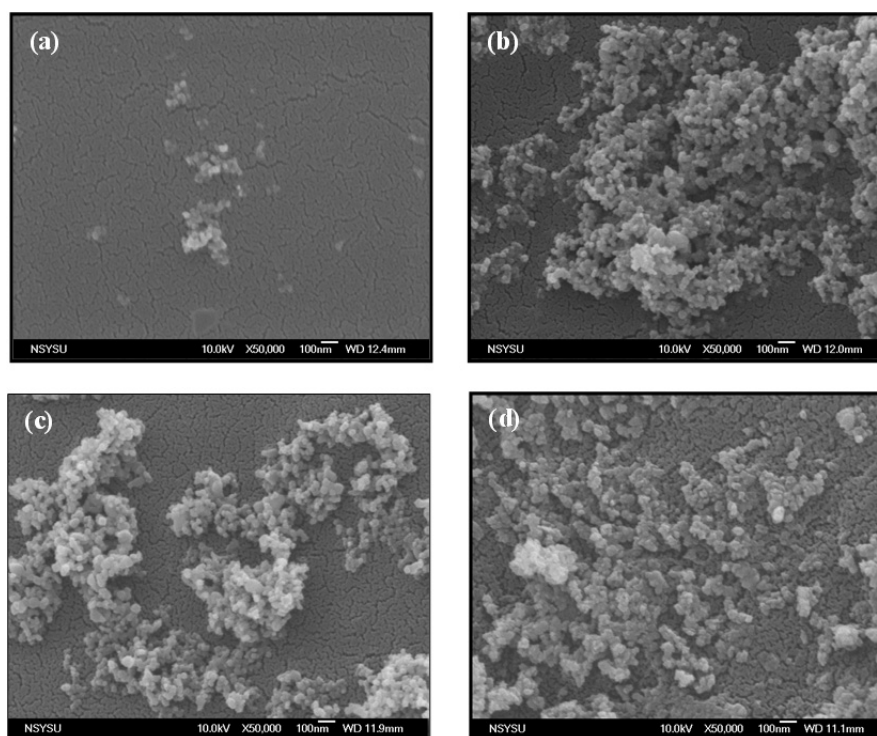


**Fig. 2.** The images of  $\text{TiO}_2$  and  $\text{Fe/TiO}_2$  coated on the surface of fiberglass by using scanning electron microscope (SEM) of fifty thousand magnifications. (a)  $\text{Fe/TiO}_2$ , (b) 1% $\text{Fe/TiO}_2$ , (c) 3% $\text{Fe/TiO}_2$ , and (d) 5% $\text{Fe/TiO}_2$ .

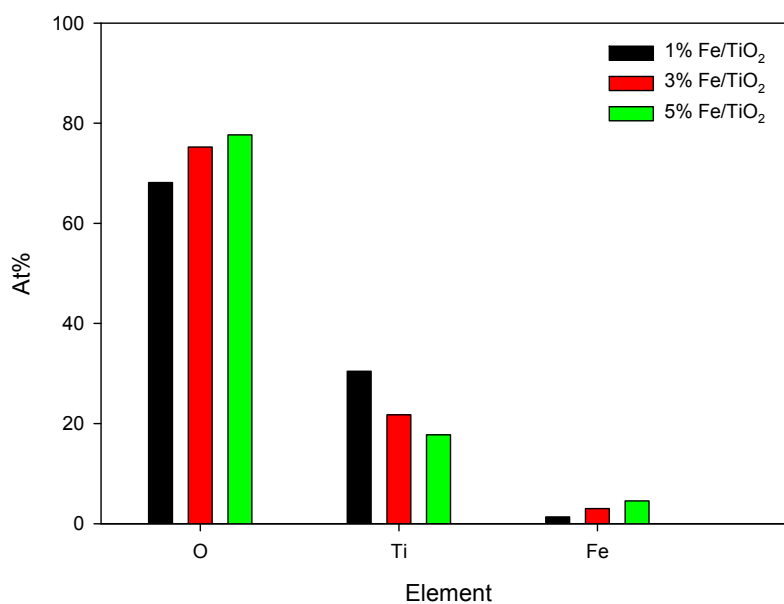


**Fig. 3.** EDS analytical results of elemental abundance for modified iron-doped  $\text{Fe/TiO}_2$  photocatalysts.

the modified photocatalyst doping with 1, 3, and 5%  $\text{Fe/TiO}_2$  photocatalysts, respectively, which concurred quite well with each other.

The absorption spectra of iron-doped  $\text{TiO}_2$  ( $\text{Fe/TiO}_2$ ) coated on the surface of fiberglass were further analyzed by UV-Vis spectrophotometer. The results showed that  $\text{Fe/TiO}_2$  had significantly photocatalytic effect on the absorbance of lights with different wavelengths. Fig. 4 shows a significant red shift of iron-doped  $\text{TiO}_2$  compared

to the commercial Degussa P-25. With the increase of iron doping percentages from 1% to 5%  $\text{Fe/TiO}_2$ , the absorbance of the UV to near-UV region (230–400 nm) increased approximately 0.9 absorbance, while that of the visible region (400–750 nm) increased about 0.8 absorbance. The results showed that the  $\text{Fe/TiO}_2$  photocatalysts irradiated by the near-UV region (300–400 nm) had better absorbance, but doping with iron could significantly enhance its absorbance of visible region.

Owing to the formation of hydroxyl radicals ( $\bullet\text{OH}$ ), electron paramagnetic resonance (EPR) spectroscopy showed that the peak-valley difference increased the amount of  $\bullet\text{OH}$  to highly enhance the decomposition efficiency of formaldehyde. However, the radicals of  $\text{Ti}^{4+}$  tended to reduce with illumination time as the signal strength decreased gradually. As shown in Fig. 5, the spectral height in the electron paramagnetic resonance (EPR) spectroscopy increased significantly with the modified  $\text{TiO}_2$  photocatalysts doped with different iron contents, indicating the increase of formaldehyde decomposition efficiency with the iron-doped content of  $\text{Fe}/\text{TiO}_2$  as shown by UV-Vis light absorption signal (Li et al., 2015).

#### Effects of Influent Formaldehyde Concentration

This study investigated the influences of influent formaldehyde concentration on the decomposition efficiency of formaldehyde. The formaldehyde decomposition experiments were conducted under the following experimental condition: the influent formaldehyde concentrations of 0.15, 0.30, and 0.45 ppm; the reaction temperature of  $25^\circ\text{C}$ ; the gas pressure of 1.0 atm; the duration of 60 min; the relative humidity of 5%, the 1%

$\text{Fe}/\text{TiO}_2$  coated fiberglass; and the irradiation of UV light ( $\lambda = 254 \text{ nm}$ ).

The adsorption of formaldehyde on the inner wall of the two reactors without UV and  $\text{O}_3$  has been conducted as a pre-experiment. The operating parameters for the formaldehyde adsorption experiments were set as follows: the inlet formaldehyde concentration of 0.3 ppm, the reaction temperature of  $25 \pm 2^\circ\text{C}$ , the gas pressure of 1.0 atm, and the reaction time of 120 min. The formaldehyde concentration was detected at the intervals of 5 min. The results of formaldehyde adsorption are shown in Fig. 6. There was no decrease of the formaldehyde concentration during the adsorption process, indicating that formaldehyde was hardly to be removed solely by adsorption process.

The simulated indoor formaldehyde of fixed concentration was generated by heating a formaldehyde permeation tube at  $50^\circ\text{C}$ , properly mixed with nitrogen gas in a mixing chamber. The stability of the influent formaldehyde concentration was carefully checked in a pre-experiment. The results of the stability experiments for different influent formaldehyde were illustrated in Fig. 7. It showed that the influent formaldehyde concentration were stable after 5 min. All formaldehyde decomposition experiments

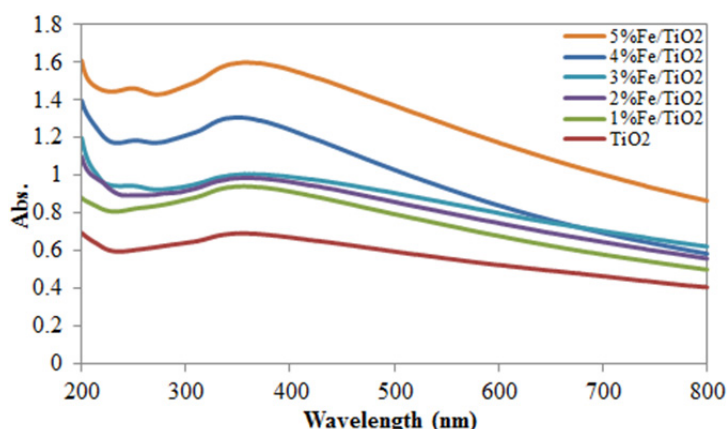


Fig. 4. UV-Vis spectrum analysis of  $\text{TiO}_2$  and 1–5%  $\text{Fe}/\text{TiO}_2$  photocatalysts.

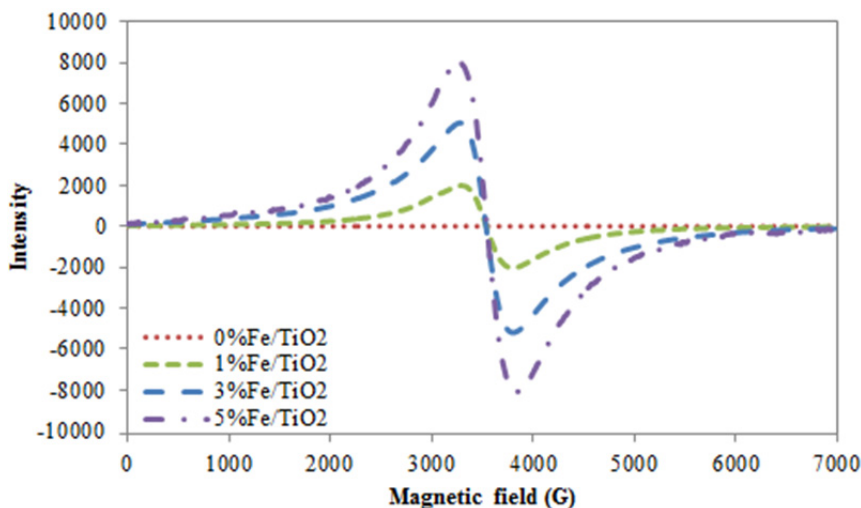
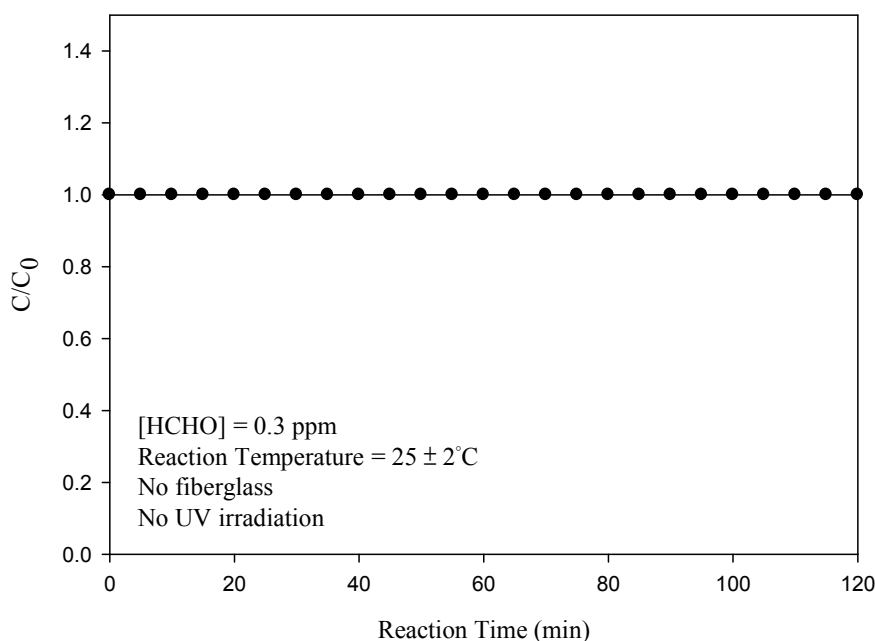
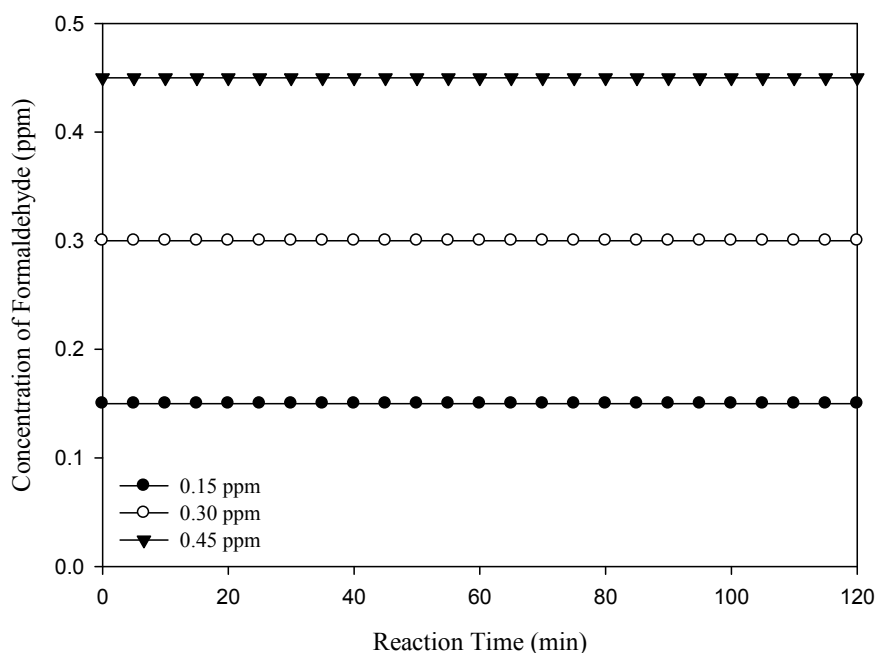


Fig. 5. EPR analysis of  $\text{TiO}_2$  and 1–5%  $\text{Fe}/\text{TiO}_2$  photocatalysts.



**Fig. 6.** Adsorption of formaldehyde in the two reactors.



**Fig. 7.** Stability of the formaldehyde concentration.

would not be conducted until stable influent formaldehyde concentrations were reached. In order to obtain stable influent formaldehyde concentration, the operation parameters including the heating temperature of the permeation tube, and the flow rate of the purged nitrogen gas used to carry the formaldehyde into the reaction system were strictly controlled.

As illustrated in Fig. 8, the decomposition efficiencies of formaldehyde were 60, 52, and 40% when the influent formaldehyde concentrations were 0.15, 0.30, and 0.45 ppm, respectively. The results indicated that the decomposition

efficiency of formaldehyde decreased as the influent formaldehyde concentration increased. The reduction of formaldehyde decomposition efficiency was probably attributed to the fact that formaldehyde molecules can diffuse faster to the surface of Fe/TiO<sub>2</sub> due to high concentration gradient of formaldehyde, however they cannot be decomposed as fast as expected at the active sites on the surface of Fe/TiO<sub>2</sub> due to the limitation of the amount of active sites. The results highly concurred with previous studies (Charuwan *et al.*, 2012; Darvishi Cheshmeh Soltani *et al.*, 2015), showing that the decomposition

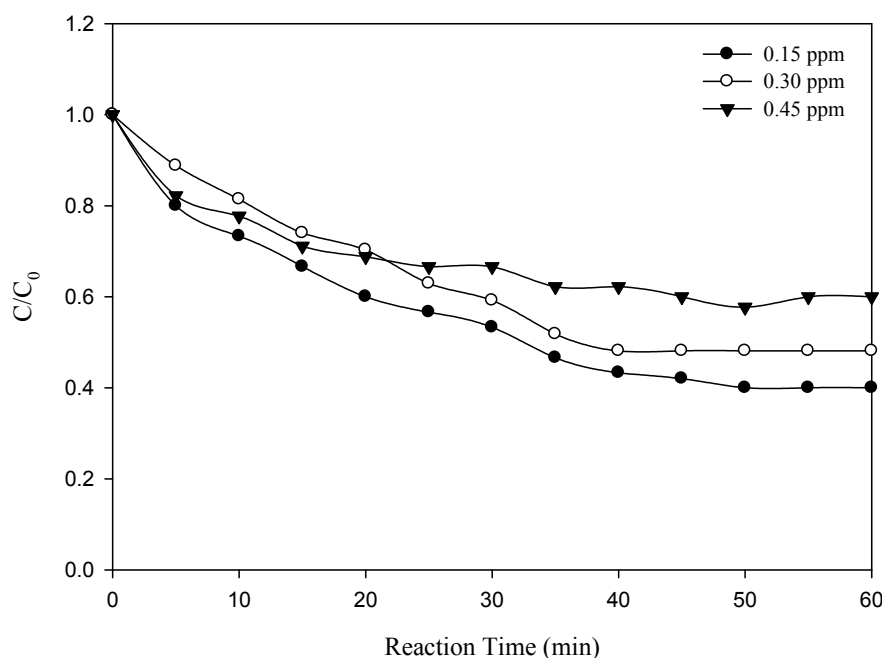


**Fig. 8.** Effects of influent formaldehyde concentration on the decomposition efficiency of formaldehyde.

efficiency of formaldehyde decreased when the initial formaldehyde concentration increased. Moreover, the reaction rate constant ( $k$ ) estimated from the pseudo-first-order reaction model was  $0.0176 \pm 0.0007 \text{ sec}^{-1}$ .

#### Effects of Relative Humidity (RH)

The relative humidities selected for this study were in the range of 20–60% since the conditioned indoor relative humidities were about 30–60%. As shown in Fig. 9, during the photocatalytic reaction process,  $\text{H}_2\text{O}$  molecule was served as an electron hole capture agent that reacted with the captured photo-generated holes and formed hydroxyl radicals ( $\bullet\text{OH}$ ). Hydroxyl radicals can effectively degrade formaldehyde on the surface of  $\text{Fe}/\text{TiO}_2$  photocatalysts, which has a strong oxidation capability, and thus enhanced the photocatalytic reaction rate in the presence of  $\text{H}_2\text{O}$  molecules. Formation of hydroxyl radicals is much crucial for the photocatalytic degradation of formaldehyde (Qi *et al.*, 2007; Yu *et al.*, 2014).

The experiments were conducted under the following experimental condition: the irradiation of UV light ( $\lambda = 254 \text{ nm}$ ); the relative humidities of 5, 35, and 55%; the influent formaldehyde concentration of 0.30 ppm; the reaction pressure of 1.0 atm; and the reaction temperature of  $25^\circ\text{C}$ . Experimental results indicated that the decomposition efficiencies of formaldehyde were 40, 34, and 20% when the relative humidities were 5, 35, and 55%, respectively. It showed that the decomposition efficiency of formaldehyde decreased as the relative humidity increased. When the concentration of water vapor increased, more water molecules could compete with formaldehyde molecules and were adsorbed on the surface of  $\text{Fe}/\text{TiO}_2$  photocatalysts, which hindered the degradation of formaldehyde and thus reduced its photocatalytic reaction rate. The highest formaldehyde decomposition efficiency went up to 40% at the relative

humidity of 5%.

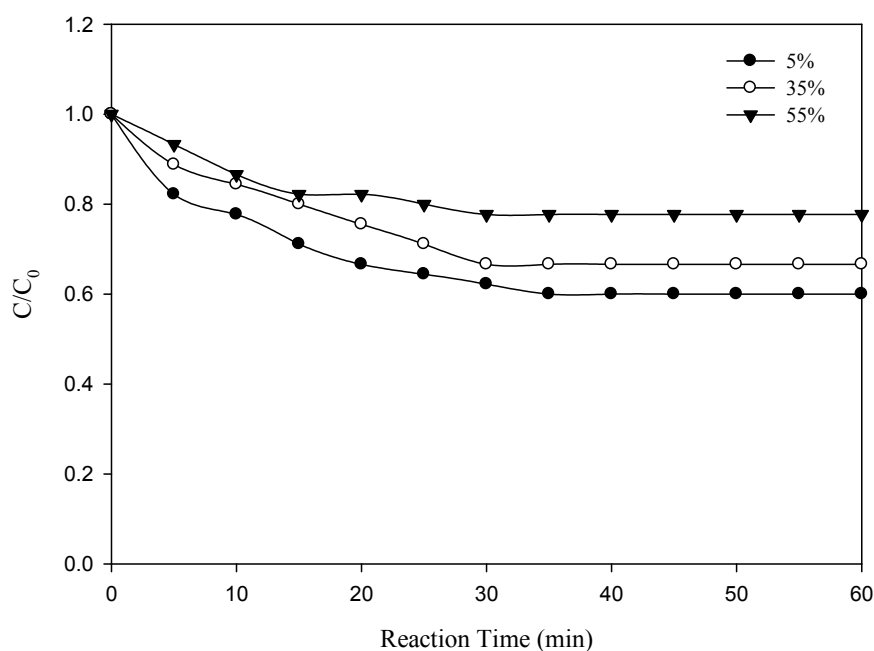
#### Effects of Reaction Temperature

In the experiments, we also investigated the effect of reaction temperature on the photocatalytic decomposition of formaldehyde under the following experimental condition: the influent formaldehyde concentration of 0.30 ppm; the reaction temperatures of 25, 45, and  $65^\circ\text{C}$ ; the reaction time of 60 min; and the irradiation of UV light ( $\lambda = 254 \text{ nm}$ ).

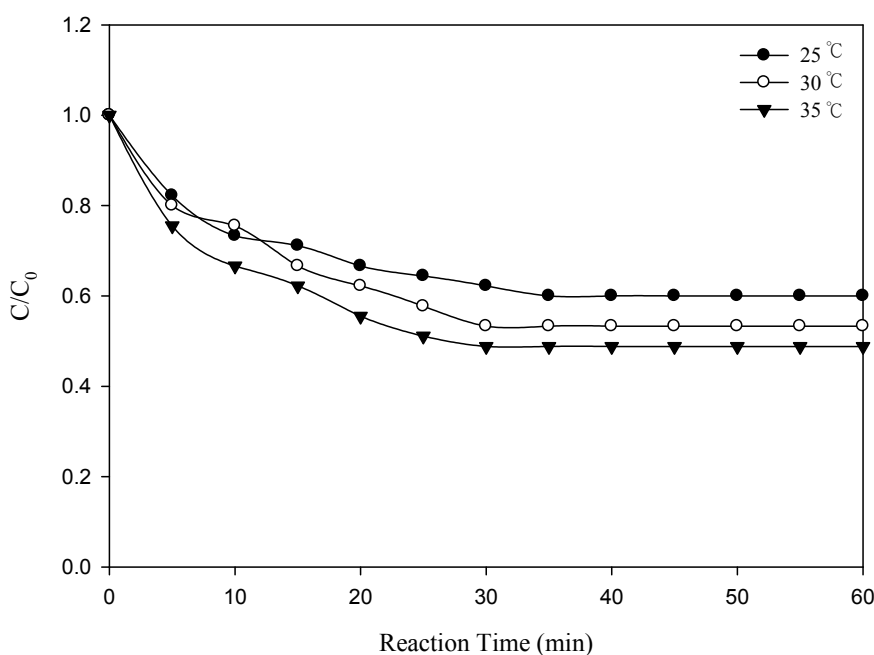
As depicted in Fig. 10, when the reaction temperatures were 25, 30, and  $35^\circ\text{C}$ , the decomposition efficiencies of formaldehyde were 40, 47, and 52%, respectively. Experimental results showed that the decomposition efficiency of formaldehyde increased as the reaction temperature increased, which followed the Arrhenius Law and concurred with previous studies (Li *et al.*, 2015; Tao *et al.*, 2015). The reaction rate constant ( $k$ ) estimated from the pseudo-first-order reaction model were 0.0167, 0.0186, and  $0.0222 \text{ sec}^{-1}$ , respectively, indicating that the reaction rate constant is proportional to the reaction temperature. Therefore, the optimal reaction temperature was  $35^\circ\text{C}$  obtained from the experimental results.

#### Effects of Incident Light Wavelength

This study further explored the photocatalytic degradation of formaldehyde under the irradiation of incident lights with different wavelengths. The experiments were conducted under the following experimental condition: the influent formaldehyde concentration of 0.30 ppm, the incident light wavelengths of visible ( $370 < \lambda < 750 \text{ nm}$ ), near-UV ( $\lambda = 365 \text{ nm}$ ), and UV ( $\lambda = 254 \text{ nm}$ ), the reaction temperature of  $25^\circ\text{C}$ , the reaction pressure of 1 atm, and the relative humidity of 5%. As illustrated in Fig. 11, the decomposition efficiencies of formaldehyde were 20, 40, and 52%, respectively, under the irradiation of visible, near-UV, and

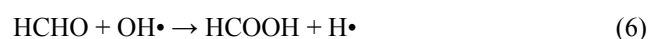
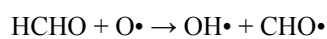
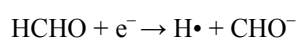
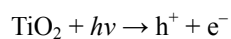


**Fig. 9.** Effects of relative humidity on the decomposition efficiency of formaldehyde.



**Fig. 10.** Effects of reaction temperature on the decomposition efficiency of formaldehyde.

UV lights. The results showed that the longer the wavelength of incident lights, the lower the decomposition efficiency of formaldehyde. The related photocatalytic reactions of formaldehyde decomposition are shown below (Liang *et al.*, 2012):



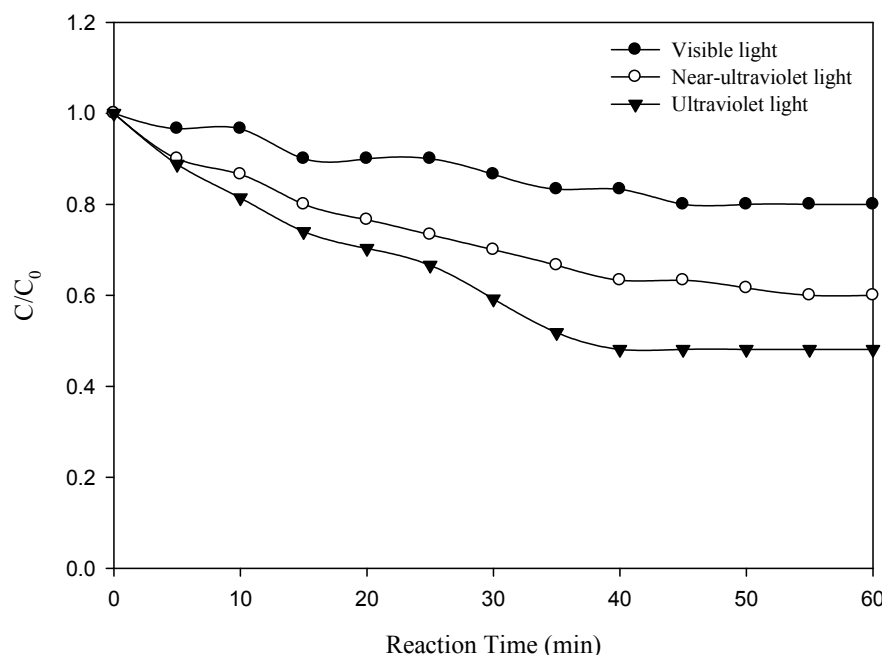


**Fig. 11.** Effects of light wavelength on the decomposition efficiency of formaldehyde.



The reaction rate constant ( $k$ ) estimated from the pseudo-first-order reaction model was  $0.0104 \pm 0.005 \text{ sec}^{-1}$ , which was mainly due to large energy gap (3.2 eV) of  $\text{TiO}_2$ . The corresponding wavelength of light was ultraviolet (Akhavan *et al.*, 2009), showing that the UV light was the optimal light source to effectively decompose formaldehyde.

#### Effects of Iron-Doped Content of $\text{Fe}/\text{TiO}_2$

The present study was also designated to investigate the influences of iron-doped content of modified photocatalyst ( $\text{Fe}/\text{TiO}_2$ ) on the decomposition efficiency of formaldehyde. The modified photocatalysts ( $\text{Fe}/\text{TiO}_2$ ) used in the experiments were the commercial  $\text{TiO}_2$  modified by doping irons with the mass ratios of 1, 3, and 5%.

Fig. 12 showed that, under the irradiation of UV light for 60 min, the decomposition efficiencies of formaldehyde were 24, 29, 36, and 45% by using  $\text{TiO}_2$  and 1, 3, and 5%  $\text{Fe}/\text{TiO}_2$ , respectively. The highest formaldehyde decomposition efficiency of 45% was obtained by using 5%  $\text{Fe}/\text{TiO}_2$ . The modified photocatalyst doped with iron ions under the ultraviolet radiation can effectively enhance the decomposition efficiency of formaldehyde. The enhancement of formaldehyde decomposition by iron-doped  $\text{TiO}_2$  ( $\text{Fe}/\text{TiO}_2$ ) may be attributed to the following facts that the doped iron ions could effectively enhance the absorption of UV-visible wavelength, increased the photocatalytic reactivity, and retarded the recombination of electron and electron-hole pair, which thus contributed to the increase of formaldehyde decomposition efficiency.

#### Effects of Injection Ozone Concentration

This study further investigated how the injection ozone concentration influenced the decomposition efficiency of

formaldehyde. The ozone concentrations injected into the photocatalytic reactor were either 2,000 or 3,000 ppb. The experiments were conducted under following experimental condition: the influent formaldehyde concentration of 0.45 ppm, the reaction temperature of 25°C, the relative humidity of 5%, the reaction pressure of 1.0 atm, and the incident of ultraviolet light ( $\lambda = 254 \text{ nm}$ ).

As shown in Fig. 13, the decomposition efficiencies of formaldehyde were 38 and 56% when the injection ozone concentrations were 2,000 and 3,000 ppb, respectively. It showed that the decomposition efficiency of formaldehyde increased with the influent ozone concentration. It was mainly attributed to higher reaction rate of formaldehyde decomposition with higher concentration of ozone, which thus accelerated the degradation of formaldehyde.

#### Photocatalytic Oxidation Combining Ozonation Oxidation ( $\text{UV}/\text{O}_3$ ) for the Decomposition of Formaldehyde

This study further investigated the overall decomposition efficiency of formaldehyde by combining photocatalytic degradation and ozone oxidation in series (i.e.,  $\text{O}_3 + \text{UV}/\text{TiO}_2$  and  $\text{UV}/\text{TiO}_2 + \text{O}_3$ ). The experiments were conducted under the following condition: the influent formaldehyde concentration of 0.45 ppm, the reaction temperature of 25°C, the relative humidity of 5%, the reaction pressure of 1.0 atm, the irradiation of ultraviolet light, and the injection ozone concentration of 3,000 ppb.

Fig. 13 illustrates that the decomposition efficiency of formaldehyde by ozone injection under the irradiation of UV light ( $\lambda = 254 \text{ nm}$ ) were 56%. It showed that the decomposition efficiencies of formaldehyde by ozone injection with and without the irradiation of UV light were exactly the same, indicating that UV light irradiation would not assist in the removal of formaldehyde in the combining

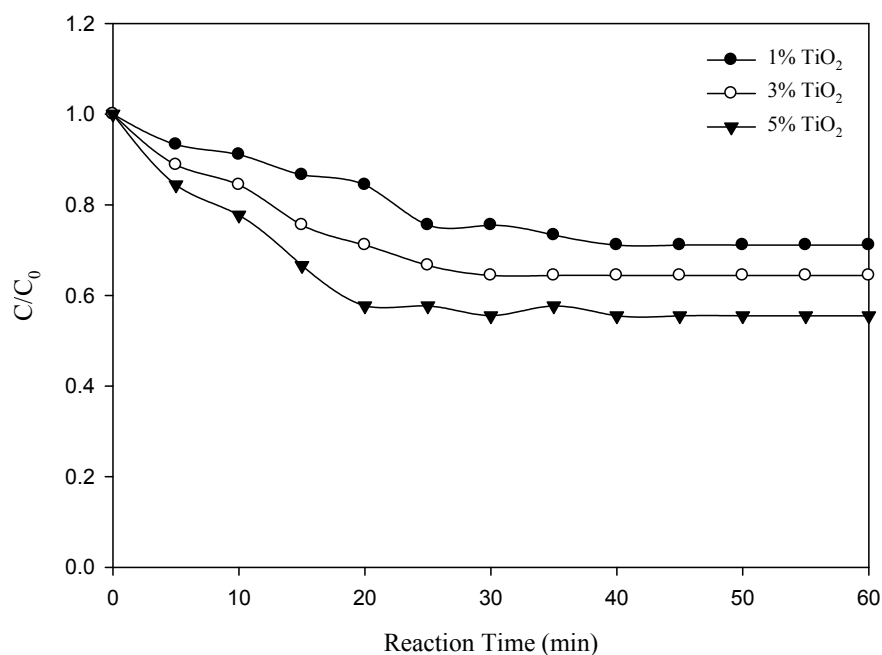


**Fig. 12.** Effects of iron doping content on the decomposition efficiency of formaldehyde.

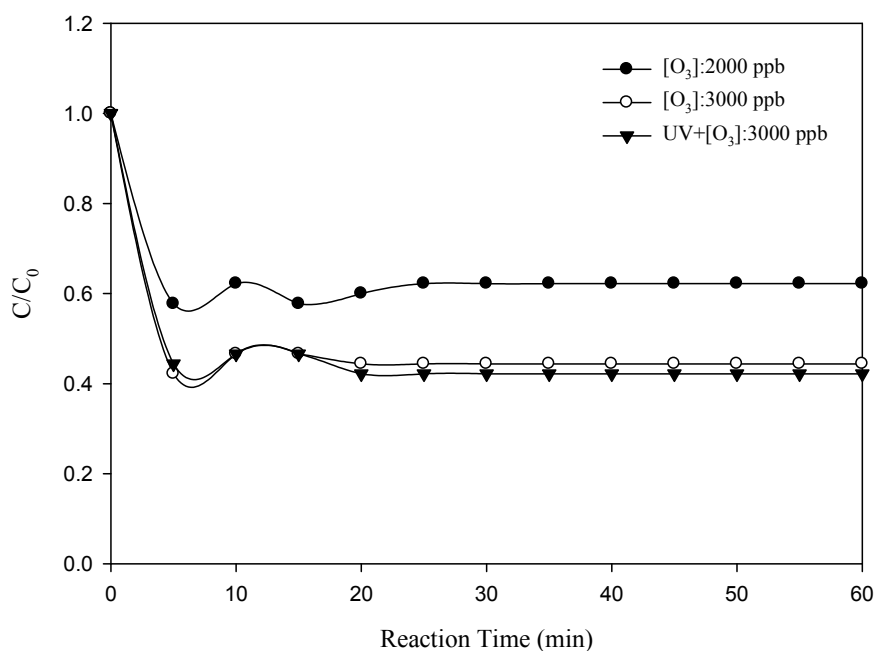
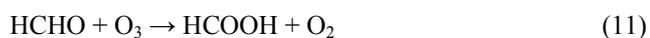


**Fig. 13.** Effects of ozone concentration on the decomposition efficiency of formaldehyde for ozone oxidation with and without the irradiation of ultraviolet light.

photocatalytic and ozonolytic reaction system. Thus, the decomposition of formaldehyde reacted with ozone can be described as follows (Esswein *et al.*, 1994):



*Decomposition of Formaldehyde by Combining O<sub>3</sub> and UV/TiO<sub>2</sub> (O<sub>3</sub> + UV/TiO<sub>2</sub>)*

In this section, the experiments were conducted under the following experimental condition: the influent formaldehyde

concentration of 0.45 ppm, the modified photocatalyst of 5% Fe/TiO<sub>2</sub>, the injection ozone concentration of 3,000 ppb. The experiments were operated in two stages (O<sub>3</sub> + UV/TiO<sub>2</sub>) with the reaction time of 120 min (Fig. 14(a)). Firstly, the formaldehyde in conjunction with ozone injection in the ozone oxidation reactor, the decomposition efficiency of formaldehyde was 56% with the reaction time of 60 min. Secondly, the remaining formaldehyde in the flow then entered the photocatalytic reactor for another 60-min photocatalytic reaction, and the photocatalytic decomposition

efficiency of formaldehyde was as low as 13%. Finally, the overall decomposition efficiency of formaldehyde went up to 69% for the  $O_3 + UV/TiO_2$  reaction system.

*Decomposition of Formaldehyde by Combining  $UV/TiO_2$  and  $O_3$  ( $UV/TiO_2 + O_3$ )*

The experiments were also conducted under the following experimental condition: the influent formaldehyde concentration of 0.45 ppm, the modified photocatalyst of 5% Fe/ $TiO_2$ , and the injection ozone concentration of 3,000 ppb. The experiments were operated in two stages ( $UV/TiO_2 + O_3$ ) with the reaction time of 120 min (Fig. 14(b)). Firstly, formaldehyde was initially decomposed

in the photocatalytic reactor and achieved its decomposition efficiency of 65% with the reaction time of 60 min. Secondly, the remaining formaldehyde in the flow then entered the ozone oxidation reactor and further reacted with the injection ozone of 3,000 ppb for another 60 min, and the decomposition efficiency of formaldehyde was 27%. The overall decomposition efficiency of formaldehyde went up to 92% for the  $UV/TiO_2 + O_3$  reaction system in series. These results concurred quite well with previous studies (Zhang *et al.*, 2003; Qi *et al.*, 2007; Lin *et al.*, 2012; Jie *et al.*, 2013) and concluded that the decomposition efficiency of formaldehyde with the  $UV/TiO_2 + O_3$  technology was 23% higher than that with the  $O_3 + UV/TiO_2$  technology.

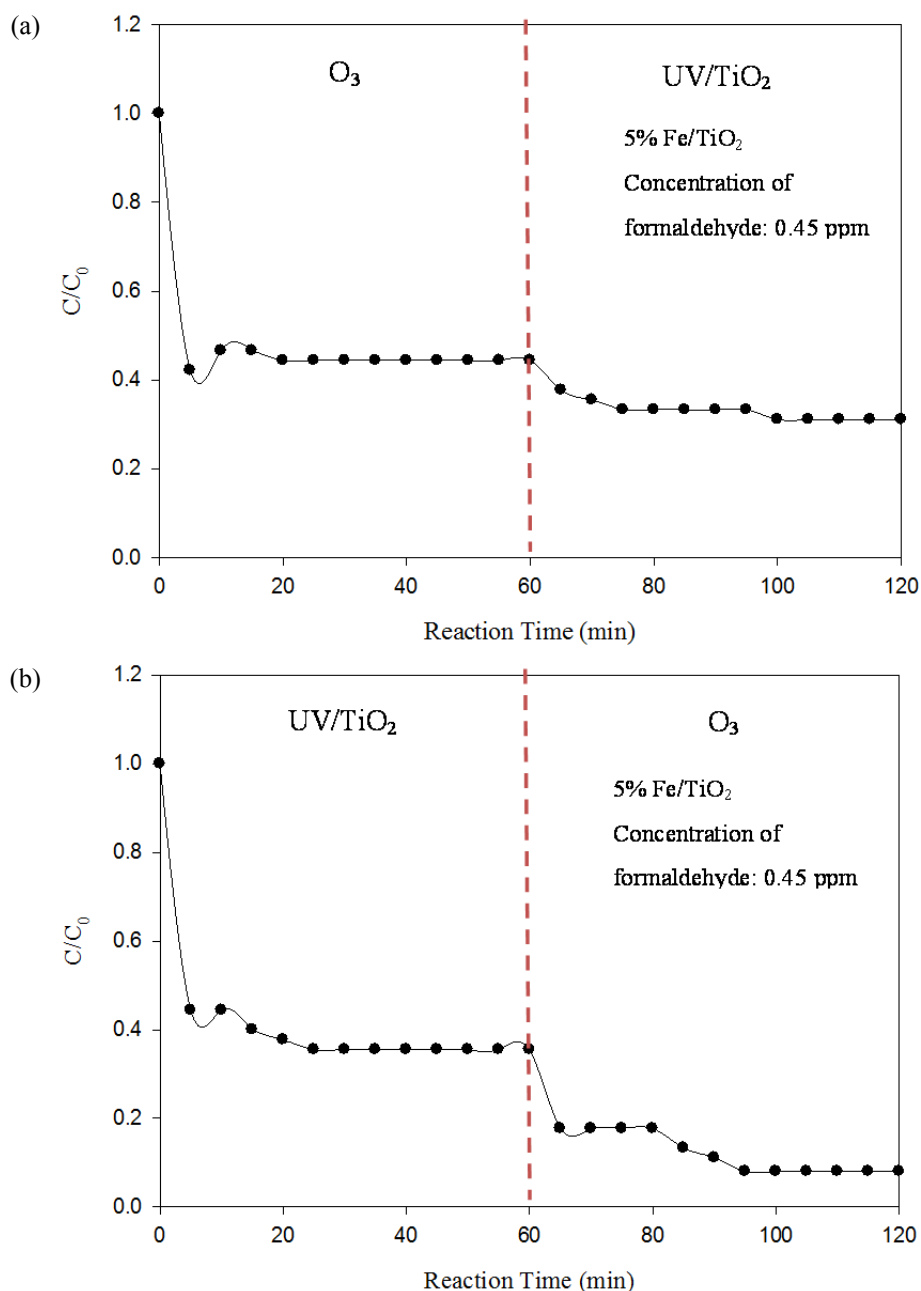


**Fig. 14.** The overall decomposition efficiencies of formaldehyde by using (a)  $O_3 + UV/TiO_2$  and (b)  $UV/TiO_2 + O_3$  reaction systems.

**Table 1.** Comparison of formaldehyde decomposition efficiencies for different oxidation techniques.

Techniques	Reaction Temperatures (°C)	Ozone Concentrations (ppb)	Relative Humidities (%)	Decomposition Efficiencies (%)
O <sub>3</sub>	25	3,000	5	56
UV/O <sub>3</sub>	25	0	5	56
O <sub>3</sub> + UV/TiO <sub>2</sub>	25	3,000	5	69
UV/TiO <sub>2</sub> + O <sub>3</sub>	25	3,000	5	92

The influent concentration of formaldehyde was 0.45 ppm for all the experiments.

A balanced chemical equation for the reaction between formaldehyde and ozone is  $\text{HCHO} + \text{O}_3 \rightarrow \text{HCOOH} + \text{O}_2$ , where formaldehyde and ozone react on a one-to-one basis yielding formic acid and oxygen. However, the formaldehyde-ozone reaction proceeds very slowly. Only part of the formaldehyde can react with ozone directly and produce formic acid. Some of the produced formic acid could be further completely oxidized to carbon dioxide and water. The residual formaldehyde and produced formic acid need to be decomposed with photocatalytic oxidation technique during the O<sub>3</sub> + UV/TiO<sub>2</sub> technique. The formic acid molecules may compete with formaldehyde molecules and lead to the decrease of formaldehyde decomposition efficiency. However, the photocatalytic oxidation technique has been widely investigated for the decomposition of formaldehyde due to its merits of complete mineralization of formaldehyde into CO<sub>2</sub> and H<sub>2</sub>O without causing secondary pollution (Qian *et al.*, 2017). The possible mechanism of the UV/TiO<sub>2</sub> + O<sub>3</sub> technique is that most of the formaldehyde could be completely mineralized to CO<sub>2</sub> and H<sub>2</sub>O, while only a little bit of formaldehyde remained in the system and further oxidized by ozone. Therefore, much more amount of formaldehyde could be decomposed during the UV/TiO<sub>2</sub> + O<sub>3</sub> process than that during the O<sub>3</sub> + UV/TiO<sub>2</sub> process.

The ozone concentration at the exit of the reaction system was also detected with an ozone detector (2B Technologies, Model 202). The ozone concentrations < 0.6 ppm were commonly observed in the exit gas of the reaction system with the UV/TiO<sub>2</sub> + O<sub>3</sub> technique. The residual ozone level may not meet the indoor air quality standards. Therefore, an after-treatment ozone decomposition catalyst might be required to diminish the residual ozone. Alternatively, the UV/TiO<sub>2</sub> combined with ozonolysis on the adsorbents is a challenge for the further investigation of formaldehyde decomposition.

## CONCLUSIONS

An innovative advanced oxidation technology combining photocatalytic degradation and ozone oxidation (UV/TiO<sub>2</sub> + O<sub>3</sub>) was successfully developed to effectively decompose indoor formaldehyde by using modified iron-doped TiO<sub>2</sub> photocatalysts (Fe/TiO<sub>2</sub>). Both TiO<sub>2</sub> and modified iron-doped TiO<sub>2</sub> (Fe/TiO<sub>2</sub>) were coated on the surface of a fiberglass filter to investigate the influence of major operating parameters (*viz.*, the influent formaldehyde concentration, reaction temperature, relative humidity, iron doping content, light irradiation, and injection ozone

concentration) on the decomposition efficiency.

Some studies have investigated the decomposition of formaldehyde using either the photocatalytic oxidation technique or the ozonization technique. However, using the photocatalytic oxidation technique followed by the ozonization technique has rarely been reported. Applying the UV/TiO<sub>2</sub> + O<sub>3</sub> reaction system increased the overall decomposition efficiency to 92%, which was higher than that of the photocatalytic oxidation process (45%) or the ozonization process (56%) alone. Therefore, the UV/TiO<sub>2</sub> + O<sub>3</sub> technique may be considered an innovative technology.

This study revealed that the decomposition efficiency of formaldehyde increased with the reaction temperature, iron doping content, and ozone injection concentration.

However, the opposite trends were observed for the influent formaldehyde concentration, relative humidity, and wavelength of the incident light. The optimal operating parameters obtained in this study were an influent formaldehyde concentration of 0.15 ppm, a relative humidity of 5%, irradiation by UV light, a reaction temperature of 35°C, an iron doping content of 5% Fe/TiO<sub>2</sub>, and an injected-ozone concentration of 3,000 ppb.

The decomposition efficiencies of formaldehyde by using four different techniques (*i.e.*, O<sub>3</sub>, UV/O<sub>3</sub>, O<sub>3</sub> + UV/TiO<sub>2</sub>, and UV/TiO<sub>2</sub> + O<sub>3</sub>) were further compared and summarized in Table 1. The highest formaldehyde decomposition efficiency, at 92%, was obtained by using the UV/TiO<sub>2</sub> + O<sub>3</sub> technology. The O<sub>3</sub> + UV/TiO<sub>2</sub> technology can achieve an efficiency of up to 69%, whereas either O<sub>3</sub> or UV/O<sub>3</sub> can achieve an efficiency of 56%. Overall, the decomposition efficiencies for different oxidation techniques were ranked as follows: UV/TiO<sub>2</sub> + O<sub>3</sub> > O<sub>3</sub> + UV/TiO<sub>2</sub> > UV/O<sub>3</sub> ≈ O<sub>3</sub>.

The maximum decomposition efficiency was obtained with an influent formaldehyde concentration of 0.45 ppm. The resulting concentration of the formaldehyde in the outlet gas of the reaction system (0.04 ppm) can meet advanced standards, and the indoor formaldehyde concentrations on site are commonly lower than 0.45 ppm. Therefore, the UV/TiO<sub>2</sub> + O<sub>3</sub> process is a promising technology for decomposing indoor formaldehyde that can potentially be applied to air cleaners designed in the future.

## ACKNOWLEDGEMENT

This study was performed under the auspices of the Ministry of Science and Technology (MOST), Republic of China, under the contract number of MOST 103-2622-E-110-006-CC3. The authors are grateful to the Ministry of Science and Technology for its constant financial support.

## REFERENCES

- Akhavan, O. (2009). Lasting antibacterial activities of AgTiO<sub>2</sub>/Ag/a-TiO<sub>2</sub> nanocomposite thin film photocatalysts under solar light irradiation. *J. Colloid Interface Sci.* 336: 117–124.
- Alberici, R.M., Canela, M.C., Eberlin, M.N. and Jardim, W.F. (2001). Catalyst deactivation in the gas phase destruction of nitrogen-containing organic compounds using TiO<sub>2</sub>/UV-VIS. *Appl. Catal. B* 30: 389–397.
- Chai, M. and Pawliszyn, J. (1995). Analysis of environmental air samples by solid-phase microextraction and gas chromatography/ion trap mass spectrometry. *Environ. Sci. Technol.* 29: 693–701.
- Charuwan, K., Kamolporn, A., Nat-a-nong, C., Kanokpun, A., Pasuree, R. and Virote, B. (2012). Photocatalytic of TiO<sub>2</sub>-SiO<sub>2</sub> thin films co-doped with Fe<sup>3+</sup> and thio-urea in the degradation of formaldehyde by indoor and outdoor visible lights. *Adv. Mater. Phys. Chem.* 2: 40–44.
- Chin, P., Yang, L.P. and Ollis, D.F. (2006). Formaldehyde removal from air via a rotating adsorbent combined with a photocatalyst reactor: Kinetic modeling. *J. Catal.* 237: 29–37.
- Darvishi Cheshmeh Soltani, R., Rezaee, A., Safari, M., Khataee, A.R. and Karimi, B. (2015). Photocatalytic degradation of formaldehyde in aqueous solution using ZnO nanoparticles immobilized on glass plates. *Desalin. Water Treat.* 53: 1613–1620.
- Delphine, B., Pierre, M., Valérie, D. and Hervé, P. (2014). Formaldehyde emission behavior of building materials: On-site measurements and modeling approach to predict indoor air pollution. *J. Hazard. Mater.* 280: 164–173.
- Esswein, E.J. and Boeniger, M.F. (1994). Effects of an ozone-generating air-purifying device on reducing concentrations of formaldehyde in air. *Appl. Occup. Environ. Hyg.* 9: 139–146.
- Gao, E., Wang, W., Shang, M. and Xu, J. (2011). Synthesis and enhanced photocatalytic performance of graphene-Bi<sub>2</sub>WO<sub>6</sub> composite. *Phys. Chem. Chem. Phys.* 13: 2887–2893.
- Hines, A.L., Ghosh, T.K., Loyalka, S.K. and Warder, R.C. (1993). *Indoor air-quality and control*. Prentice-Hall, Englewood.
- Ho, S.H., Cheng, Y., Bai, Y., Ho, K.F., Dai, W.T., Cao, J.J., Lee, S.C., Huang, Y., Ip, H.S., Deng, W.J. and Guo, W. (2015). Risk assessment of indoor formaldehyde and other carbonyls in campus environments in northwestern China. *Aerosol Air Qual. Res.* 16: 1967–1980.
- Hoffmann, M.R., Martin, S.T., Choi, W. and Bahnemann, D.W. (1995). Environmental applications of semiconductor photocatalysis. *Chem. Rev.* 95: 69–96.
- Hong, W., Meng M., Xie, J., Gao, D., Zeng, Y., Ai, H., Chen, C., Huang, S. and Zhou, Z. (2017). Investigation of the pollution level and affecting factors of formaldehyde in typical public places in Guangxi, China. *Aerosol Air Qual. Res.* 17: 2816–2828.
- Jie, S., Xin, Y., Kangle, L., Shuo, S., Kejian, D. and Dongyun, D. (2013). Photocatalytic degradation pathway for azo dye in TiO<sub>2</sub>/UV/O<sub>3</sub> system: Hydroxyl radical versus hole. *J. Mol. Catal. A: Chem.* 367: 31–37.
- Jones, A.P. (1999). Indoor air quality and health. *Atmos. Environ.* 33: 4535–4564.
- Kwon, D.W., Seo, P.W., Kim, G.J. and Hong, S.C. (2015). Characteristics of the HCHO oxidation reaction over Pt/TiO<sub>2</sub> catalysts at room temperature: The effect of relative humidity on catalytic activity. *Appl. Catal. B* 163: 436–443.
- Li, P.X., Feng, M.Y., Wu, C.P., Li, S.B., Hou, L.T., Ma, J.S. and Yin, C.H. (2015). Study on the photocatalytic mechanism of TiO<sub>2</sub> Sensitized by Zinc Porphyrin. *Acta Phys. Sinica* 64: 137601.
- Liang, W.J., Li, J. and Jin, Y.Q. (2012). Photo-catalytic degradation of gaseous formaldehyde by TiO<sub>2</sub>/UV, Ag/TiO<sub>2</sub>/UV and Ce/TiO<sub>2</sub>/UV. *Build. Environ.* 51: 345–350.
- Lin, L., Xie, M.N., Liang, Y.M., He, Y.Q., Chan, G.Y.S. and Luan, T.G. (2012). Degradation of cypermethrin, malathion and dichlorovos in water and on tea leaves with O<sub>3</sub>/UV/TiO<sub>2</sub> treatment. *Food Control* 28: 374–379.
- Qi, H., Sun D.Z. and Chi G.Q. (2007). Formaldehyde degradation by UV/TiO<sub>2</sub>/O<sub>3</sub> process using continuous flow mode. *J. Environ. Sci.* 19: 1136–1140.
- Qian, X., Ren, M., Yue D., Zhu Y., Han Y., Bian Z. and Zhao, Y. (2017). Mesoporous TiO<sub>2</sub> films coated on carbon foam based on waste polyurethane for enhanced photocatalytic oxidation of VOCs. *Appl. Catal. B* 212: 1–6.
- Romaguera, C., Grimalt, F., and Lecha, M. (1981). Occupational purpuric textile dermatitis from formaldehyde resins. *Contact Dermatitis* 7: 152–153.
- Sano, T., Negishi, N., Mas, D. and Takeuchi, K. (2000). Photocatalytic decomposition of N<sub>2</sub>O on highly dispersed Ag<sup>+</sup> ions on TiO<sub>2</sub> prepared by photodeposition. *J. Catal.* 194: 71–79.
- Tang, A.D., Jia, Y.R., Zhang, S.Y., Yu, Q.M. and Zhang, X.C. (2014). Synthesis, characterization and photocatalysis of AgAlO<sub>2</sub>/TiO<sub>2</sub> heterojunction with sunlight irradiation. *Catal. Commun.* 50: 1–4.
- Tao, H.T., Fan, Y.S., Li, X.Q., Zhang, Z.R. and Hou, W.S. (2015). Investigation of formaldehyde and TVOC in underground malls in Xi'an, China: Concentrations, sources, and affecting factors. *Build. Environ.* 85: 85–93.
- Xiong, D., Chang, H., Zhang, Q.Q., Tian, S., Liu, B.S. and Zhao, X.J. (2015). Preparation and characterization of CuCrO<sub>2</sub>/TiO<sub>2</sub> heterostructure photocatalyst with enhanced photocatalytic activity. *Appl. Surf. Sci.* 347: 747–754.
- Xu, H., Li, H., Gu, Z., Xu, Y., Yan, J., Wu, X. and Zhao, S. (2012). Photocatalytic degradation of methylene blue over AgAlO<sub>2</sub> under UV light irradiation. *J. Chem. Soc. Pakistan* 34: 371–375.
- Yu, K.P., Lee W.M. and Lin, G.Y., (2014). Removal of low-concentration formaldehyde by a fiber optic illuminated honeycomb monolith photocatalytic reactor. *Aerosol Air Qual. Res.* 15: 1008–1016.
- Yun, H.N., Akihida, I., Akihiko, K. and Rose, A. (2010). Reducing graphene oxide on a visible-light BiVO<sub>4</sub> photocatalyst for an enhanced photoelectrochemical water splitting. *J. Phys. Chem.* 17: 2607–2612.

Zeliger, H.I. (2008). 12-Sick building syndrome, In *Human toxicology of chemical mixtures*, Zeliger, H.I. (Ed.), William Andrew Publishing, Norwich, NY, pp. 175–195.

Zhang, P.Y., Liang, F.Y., Yu, G., Chen, Q. and Zhu, W.P. (2003). A comparative study on decomposition of gaseous toluene by O<sub>3</sub>/UV, TiO<sub>2</sub>/UV and O<sub>3</sub>/TiO<sub>2</sub>/UV. *J.*

*Photochem. Photobiol. A* 156: 189–194.

*Received for review, May 3, 2018*

*Revised, June 18, 2018*

*Accepted, June 24, 2018*